CHAPTER 2: PUTATIVE VOLTAGE SENSING ARGININES IN THE MECHANOSENSITIVE CHANNEL OF SMALL CONDUCTANCE (MSCS)

2.1 Introduction

2.1.1 Mechanosensitive channels are ubiquitous across species

The ability of a cell to detect changes in its mechanical environment underlies a myriad of physiological processes including touch and pain sensation,[1-3] gravity detection, blood pressure control,[4] hearing and vestibular function,[5-7] tissue growth,[8] cell volume control,[9-11] and osmoregulation.[12] Additionally, mechanosensors have been suggested to play roles in neuronal development and plasticity as well as stress and inflammation. Given the vast roles of mechanosensitive mechanisms in physiological processes, it is not surprising that the disruption of these mechanosensitive mechanisms have been suggested to contribute to a variety of maladies such as neuronal and muscular degeneration,[13, 14] cardiac arrhythmias,[15-17] and hypertension,[18] arteriosclerosis,[19] and glaucoma.[20] In the past several decades, the molecular mechanisms underlying specific mechanosensitive processes have been identified. They include mechanosensitive channels,[21-23] mechanosensitive receptors,[24, 25] enzymes,[26, 27] and transmitter release.[28]

Mechanosensitive channels are integral membrane proteins that open and close in response to mechanical stress applied directly to the cell membrane or through indirect means via cytoskeletal components.[29-31] Mechanosensitive channels transduce a mechanical signal into an electrochemical response, thus allowing a cell to respond to stimuli such as sound, touch, gravity and pressure. They have been found in all branches of the phyllogenetic tree—*Eubacteria*, *Eukaya*, and *Archaea* and exhibit vast diversity both physiologically and structurally.[32] Eukaryotic mechanosensitive channels include the transient receptor potential vanilloid (TRPV) subclass of the Transient Receptor Potential

(TRP) channel family,[33] the TREK-1 and TRAKK members of the potassium channel family K_{2p},[34, 35] and the DEG/ENaC superfamily.[36, 37]

Given the role of mechanosensitive channels in a variety of biological processes, it is of interest to understand how these channels function. Unfortunately, eukaryotic mechanosensitive systems tend to be complex, involving multiple components, and as such they have yet to be well characterized biochemically. Prokaryotic mechanosensitive channels, on the other hand, can be relatively simple and tend to be intrinsically mechanosensitive, making them attractive model systems for studies on mechanosensation. Furthermore, prokaryotic mechanosensitive systems are significantly more amenable to genetic manipulations; hence more facile for biochemical and biophysical characterization. As a result, a wealth of information has been obtained through the study of prokaryotic mechanosensitive channels which might be relevant to the more complex eukaryotic mechanosensitive systems.

2.1.2 Prokaryotic mechanosensitive channels

First discovered in giant spheroplasts of bacteria, prokaryotic mechanosensitive channels are thought to function in the maintenance of cell turgor, acting as "emergency release valves" in the event of a sudden increase in external osmolarity.[38-42] There are three mechanosensitive proteins known to be associated with the mechanosensative channel activities of *E. coli*—the mechanosensitive channel of mini conductance (MscM),[43] the mechanosensitive channel of small conductance (MscS),[38, 43] and the mechanosensitive channel of large conductance (MscL).[44] These channels were characterized by their conductance and sensitivity to applied pressure with *in situ* and *in vitro* recordings

demonstrating that increased conductance correlated to a higher activation pressure. The conductance of MscL was shown to be between 2.5 and 3 nS whereas MscS has a conductance of 1 nS.[45, 46] Under osmotic stress, MscM opens first in attempts to maintain cell turgor followed by the opening of MscS should the gating of MscM not be sufficient. MscL acts as a last resort in response to sudden changes in external osmotic stress. MscL has been proposed to share an evolutionary origin with the sensor module of the eukaryotic, voltage-gated TRP channels as well as polycystin channels. Electrophysiological analysis of MscS activity was later shown to be the sum of the two channels KefA and YggB; however, reconstitution of YggB alone exhibited MscS conductance.[47, 48] Therefore, YggB became known as MscS and KefA was renamed MscK due to its interaction with K^+.[49] MscS and MscK share homology with each other and both have been proposed to be distantly related to MscL, although neither show strong homology with MscL.[50]

2.1.2.1 The mechanosensitive channel of small conductance

The mechanosensitive channel of small conductance (MscS) is characterized by a conductance of 1 nS and is opened with moderate pressure. The pressure threshold of opening for MscS was shown to be approximately 50% that of MscL.[22, 51] When first analyzed by electrophysiological analysis, MscS activity in *E. coli* was attributed to the sum of two channels, KefA and YggB. Booth and co-workers identified the protein YggB, which is 286 amino acids in length, as being necessary for MscS activity whereas deletion of the KefA gene appeared to be without a phenotype.[52] KefA was subsequently renamed MscK. KefA contains a domain highly homologous to YggB at the C-terminal tail of the protein and encodes a channel that displays MscS-like activity. Once the gene responsible for MscS was

discovered, it allowed for searches of genomic databases for homologous channels. The result of sequence homology searches has suggested that the MscS family is much larger and variable in size and sequence than the MscL family. MscS homologues appear to be prevelant in *Archaea* as well as eukaryotes.

Unlike MscL, MscS is not only mechanosensitive but it is also voltage modulated. The open probability of MscS increases *e*-fold for each +15 mV increase in membrane depolarization.[38] This is equivalent to the movement of 1.7 charges across the membrane during a gating event. MscS also shows a slight anion preference, although it is largely nonselective.[48, 50, 53] Mutational analysis suggests that MscS will tolerate minor mutations to the N-terminal region, however the C-terminal domain appears to be critical for its stability.[54]

2.1.2.2 Crystal structure of E. coli mechanosensitive channel of small conductance (MscS)

In 2002, the Rees group successfully obtained a crystal structure of *E. coli* MscS at 3.9 Å resolution.[55] The crystal structure represents the first structural look at a voltage-modulated ion channel. The 3.9 Å structure established that the channel assembled as a homoheptamer and could be divided into two regions—an extramembrane and transmembrane region (Figure 2.1). It is likely that the extramembrane region is cytoplasmic and the N-terminal region of MscS is periplasmic. The extramembrane region can be further divided into two domains that Bass *et al.* describe as the middle-beta domain and the carboxy-terminal domain. The channel spans approximately 120 Å in the direction parallel to the sevenfold axis with the extramembrane domain contributing 70 Å in length and the transmembrane domain contributing approximately 50 Å. The width of the channel in the direction perpendicular to the sevenfold axis spans approximately 80 Å.

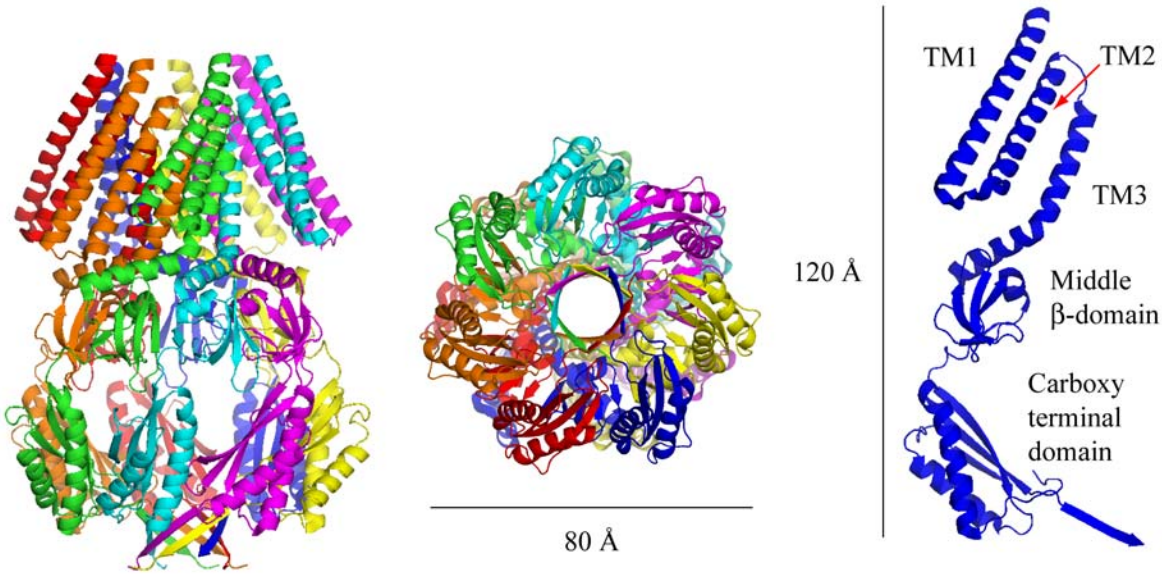

Figure 2.1. Crystal structure of MscS.

A channel is formed from helices from the membrane spanning region of each subunit that opens into a 40 Å chamber formed by the extramembrane regions. Interestingly, this chamber is connected to the cytoplasm through eight openings in between the middle-beta and carboxy-terminal domains of each subunit—seven openings on the sides of the chamber and a single opening at the bottom of the channel. The structural arrangement of MscS bares no resemblance to that of MscL or any other structural characterized channels.

Examination of each individual subunit that forms MscS reveals the transmembrane domain is comprised of three helices, TM1, TM2, and TM3. TM1 contains amino acids 29 to 57, TM2 is made of residues 68 to 91 and TM3 consists of residues 96 to 127. A prominent kink is present at glycine 113 within the TM3 region, presumably marking the membrane boundary of MscS. The pore of the channel is predominantly formed from the residues prior to this kink (residues 96 to 113) of TM3. The middle-beta domain, consisting

of residues 132 to 177, contains five beta-strands. The beta-strands of one subunit pack with those from other subunits to form a beta barrel like structure around the protein. The carboxy-terminal end of the protein exhibits a mixed alpha/beta structure and forms seven of the openings with the middle-beta domain, each with a diameter of approximately 14 Å. Because the structure reveals a permeation pathway that resembles a tapered cylinder with a diameter of 10 Å at the narrowest point, Bass *et al.*, propose that the crystal structure is most likely that of the open state of MscS.

2.1.2.3 Putative arginines in the voltage sensing mechanism of E. coli mechanosensitive channel of small conductance (MscS)

The crystal structure of MscS has several implications for the gating of MscS. In particular, the mechanism by which MscS is voltage modulated may be relevant to other voltage sensitive channels. The voltage sensitivity of K_v channels is conferred by a series of positively charged residues dispersed along the S4 helix. Most of these charged residues are arginines. The crystal structure of MscS reveals three arginines that may be appropriately positioned such that they could act as the voltage sensor in the voltage modulated gating of MscS (Figure 2.2). Arginine 46 and arginine 74 are located in TM1 and TM2 of MscS; TM1 and TM2 are adjacent to the permeation pathway and Bass *et al.* suggest they are likely candidates as mediators of the conformation change that occurs in MscS in response to applied tension or membrane depolarization. Therefore, the positions of Arg46 and Arg74 are such that their movement in response to changes in membrane potential could be translated into the opening and closing of the permeation pathway.

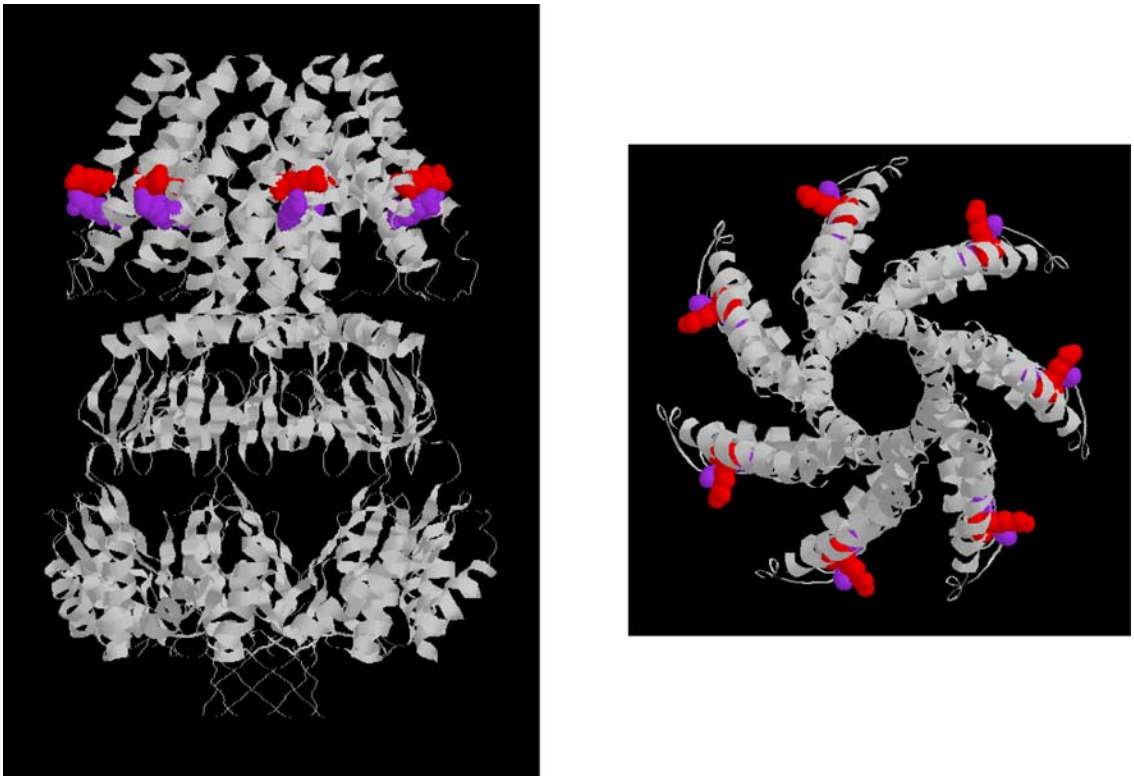

Figure 2.2. Putative voltage sensing arginines in MscS. Arg46 is shown in red and Arg 74 is shown in purple.

2.1.3 Voltage-gated ion channels

Electricity has a ubiquitous role in biology. The flow of ions through an ion channel and thus across a membrane constitutes an electrical current which results in a voltage difference across the membrane. All living cell have evolved the ability to exploit transmembrane electrical potentials in a myriad of biological processes through the use of voltage-gated ion channels. In particular, the group of "excitable cells" that includes neurons, muscle cells and endocrine cells extensively utilizes voltage-gated ion channels for fast electrical signaling. In neurons, electrical impulses result from action potentials, which are spike like changes in voltage across the membrane. They are millisecond long and are

capable of propagating at a rate of meters per second along a nerve fiber. Action potentials arise from the flow of various ions out of or into cells via membrane spanning ion channels that are voltage dependent. The ability to sense and respond to voltage is the key feature of voltage-gated ion channels that allow for the propagation of electrical signals in the nervous system and thus allows for the vast variety of firing patterns that are required for the processing of sensory information and generating motor outputs.

Hodgkin and Huxley were first to demonstrate the presence of voltage-activated sodium and potassium ion channels in the axon of a giant squid.[56-62] They showed that action potentials were made possible by a feedback process in which the direct action of voltage on ion channels resulted in channel gating and thus flow of ions. Sodium channels opened (activated) in response to a positive voltage, serving as the positive feedback segment. This is followed by the activation of potassium channels which serves as the negative feedback element. In essence, they demonstrated that there had to be charges or charge dipoles in the membrane that move in response to changes in voltage across the membrane thus turning the sodium and potassium ion channels on and off.

Voltage-gated channels share three defining features: 1) a pore forming domain that contains the permeation pathway and channel gates that control the flow of ions through the pore, 2) a voltage-sensing domain that contains the structural element that has the ability to respond to changes in transmembrane potential; also known as the voltage sensor and 3) a coupling element that links the voltage-sensing domain to the gates of the pore such that a change in transmembrane potential, and thus a response by the voltage-sensing domain, results in movement of the channel gates allowing ions to permeate the channel.

Since Hodgkin and Huxley's first voltage-clamp experiments were performed in 1952, an enormous effort has been put forth attempting to elucidate how voltage-gated ion channels work—both in how voltage causes the opening and closing of the channel and the coupling mechanism between the voltage sensor and the gate of the channel.

2.1.3.2 Voltage-gated potassium (K_v) ion channels

Much of what is known regarding the mechanism of gating for voltage-gated ion channels has come from the studies of the family of voltage-gated potassium channels (K_v). Voltage-gated potassium channels (K_v) channels are the prototypical voltage-gated channels and, as with voltage-gated Na^+ and Ca^{+2} channels, there is an enormous variety within its family. The K_v channel family is made up of over twenty-two different genes in mammals, with greater variations occurring from alternative splicing and heteromultimerization.

The basic channel architecture of the prototypical K_v channel is depicted in Figure 2.3.[63-65] They are typically tetrameric channels with each subunit containing a voltage sensor and a pore lining domain to contribute to the channel pore. A standard K_v channel subunit consists of six transmembrane domains (S1-S6) with both the amino- and carboxy-termini residing on the intracellular side of the membrane. The S5 and S6 segments comprise the pore forming domain. The narrowest part of the pore, the selectively filter, is formed by a loop between S5 and S6. The S4 domain contains multiple positively charged residues and contains the voltage sensor. K_v channels exhibit extremely high selectivity for the ions that are allowed to permeate, yet have transport rates that are close to the aqueous diffusion limit. High speed of ion transport and selectivity are critical in allowing these channels to accurately produce the rapid voltage changes necessary for action potentials in neurons

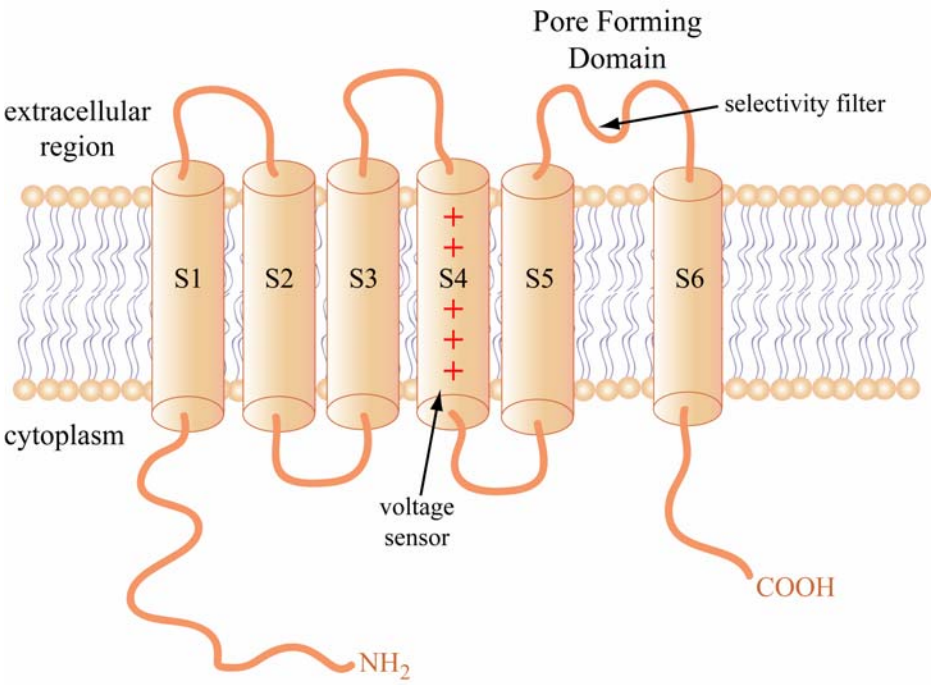

Figure 2.3. Schematic of a K_v channel subunit.

without the use of millions of proteins. The structural features that allow for a high speed of ion transport and ion selectivity have been well characterized.[66-69] The selectivity filter architecture will not be discussed here, however a number of reviews have been published that include discussion of the selectivity filter of K_v channels.[70-74]

2.1.3.3 Mechanisms of gating of voltage-gated potassium channels

While much is known about the architectural features that contribute to the high selectivity and rate of ion permeation of K_v channels, less is known about the mechanisms that govern the gating of K_v channels. A great deal of interest lies in understanding how a voltage-gated ion channel translates a change in membrane potential into a conformational change that results in channel gating. Understanding the gating mechanism involves three elements—1) the conformational change around the pore that occurs during its opening and

closing, 2) the movement of the voltage sensor in response to a change in membrane potential, and 3) the coupling between the voltage sensor and then pore that translate movement of the voltage sensor into conformational changes of the pore such that the pore opens or closes.

2.1.3.4 Mechanisms of pore closing in K_v channels

There are three proposed mechanisms by which the pore of voltage-gated K^+ channels close. Two mechanisms involve conformational changes such that a constriction occurs in the permeation pathway and the other involves obstruction of the pore by an inhibitory portion of the channel protein. The first mechanism of pore closing involves a "pinching" of the pore via movement of the S6 bundle, in which the S6 bundle moves such that it obstructs entrance to the water filled cavity via movement of the bottom ends (intracellular) of the S6 helices to form a "bundle crossing." This mechanism is supported by the interaction of ion channel blockers with the pore and the trapping of ion channel blockers within a cavity.[75, 76] It is also supported by high sequence conservation of the S6 transmembrane and intracellular portion among the principle families of voltage-gated K^+ channels—in particular, a highly conserved proline sequence (PxP or PxG) that may serve as a hinge.[77-79]

The second mechanism of inactivation is known as N-type inactivation, or the ball-and-chain mechanism, and does not involve pore constriction. Rather a physical obstruction of the pore by the N-terminus of one of the channel subunits is involded. N-type inactivation can be disrupted by enzymatic cleavage or by genetic removal of the N-terminus of the channel and can be restored by the addition of a soluble peptide derived from the N-terminus from an N-type inactivating channel.[80-83] It should be noted that there is little sequence

consensus among N-terminal portions that are capable of N-type inactivation, however it appears as though positive charge and hydrophobic character are important for the interaction of the N-terminus with the open pore of the channel.[82, 84]

The third mechanism by which the pore of a K_v channel can close involves the pinching of the selectivity filter itself, known as C-type inactivation. This type of interaction was observed in Shaker K^+ channels that had the N-terminal blocking peptide removed. This type of mechanism has been supported by various studies.[85-89] In particular, Yellen *et al.,* showed that once this type of inactivation occurred, it could be locked shut by a metal ion bridging cysteines that had been introduced into each subunit.[88] Furthermore this type of inactivation can be prevented by locking the selectivity filter open with the addition of extracellular tetrabutylammonium ion.[90]

2.1.3.5 Mechanisms of voltage-sensation and translation into pore gating

An area of enormous interest has been in understanding the movement of the voltage sensor and how its movement is coupled to the gating of the pore.[91-94] Fifty years of biophysical studies supported two main models—the helical screw model and the transporter model (figure 2.4(A) and 2.4(B)). The helical screw model posits that the S4 segment of each subunit rotates upon depolarization.[95-99] As the S4 segment rotates on its axis, it also translates perpendicular to the membrane such that it is exposed to the extracellular solution, thus moving the intracellular charges. This movement effectively translocates 4 e_0 per subunit across the membrane. In the transporter model, the translocation of charges is achieved by the tilt and rotation of the S4 segment. In the closed state, the charges occupy a water crevice exposed to the intracellular solution. The tilt and rotation of the S4 segments

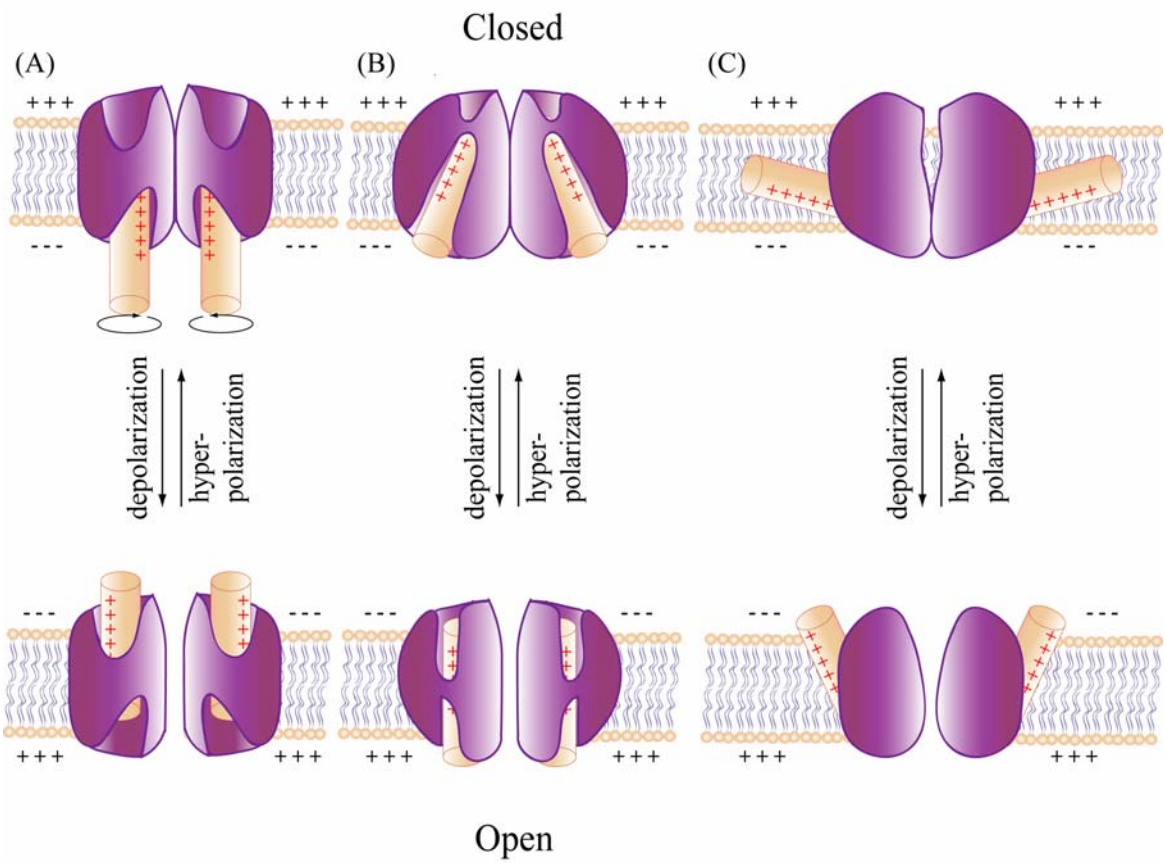

Figure 2.4. Three models of voltage sensing in voltage-gated ion channels. (A) Helical screw model, (B) transporter model, (C) paddle model.

to the open position results in the charges occupying another water crevice that exposes them to the extracellular solution.[92, 100]

In 2003, the MacKinnon group introduced a model that is dramatically different from the helical-screw and transporter models.[101, 102] The crystal structure of K_vAP coupled with data from biotin and streptavidin "scanning" experiments support a "paddle" model in which the S4 segment is located in the periphery of the channel with the charges embedded in the membrane bilayer (figure 2.4(C)). Depolarization results in a large translation of the S4 segment such that the charges go from being embedded in the bilayer in the closed state to

being exposed to the extracellular solution in the open state. This model has raised many questions given its stark difference to the helical-screw and transporter models.[103, 104]

2.2 Experimental design

The focus of the research described herein was to elucidate the role of arginine 46 and arginine 74 in the voltage sensitivity of MscS. The method to elucidate the role of these putative arginines in voltage sensation is relatively straightforward. Conventional mutagenesis was used to separately mutate each arginine amino acid to alanine residues, effectively removing the putative contribution of that particular arginine to the voltage sensitivity of MscS. The mutant channel was then expressed in *E. coli*. The cultures were used to generate giant *E. coli* spheroplasts for single channel analysis by cell-detached patch clamp electrophysiology. If either or both arginines contribute to the voltage sensitivity of MscS then we expect the dependence of the open probability of the mutant MscS on membrane depolarization to be diminished.

2.3 Results

2.3.1 Spheroplasts preparation

E. coli spheroplasts were generated using a standard established procedure with slight modifications.[45, 105] Spheroplasts allow for the use of bacterial systems for patch clamp. Bacteria are typically 1 μm in diameter, which is the approximate size of the electrode tip; therefore bacteria cannot be used to form a patch for electrophysiological analysis. Spheroplasts range in diameter from 6 to 10 μm and are the appropriate size for patch formation.

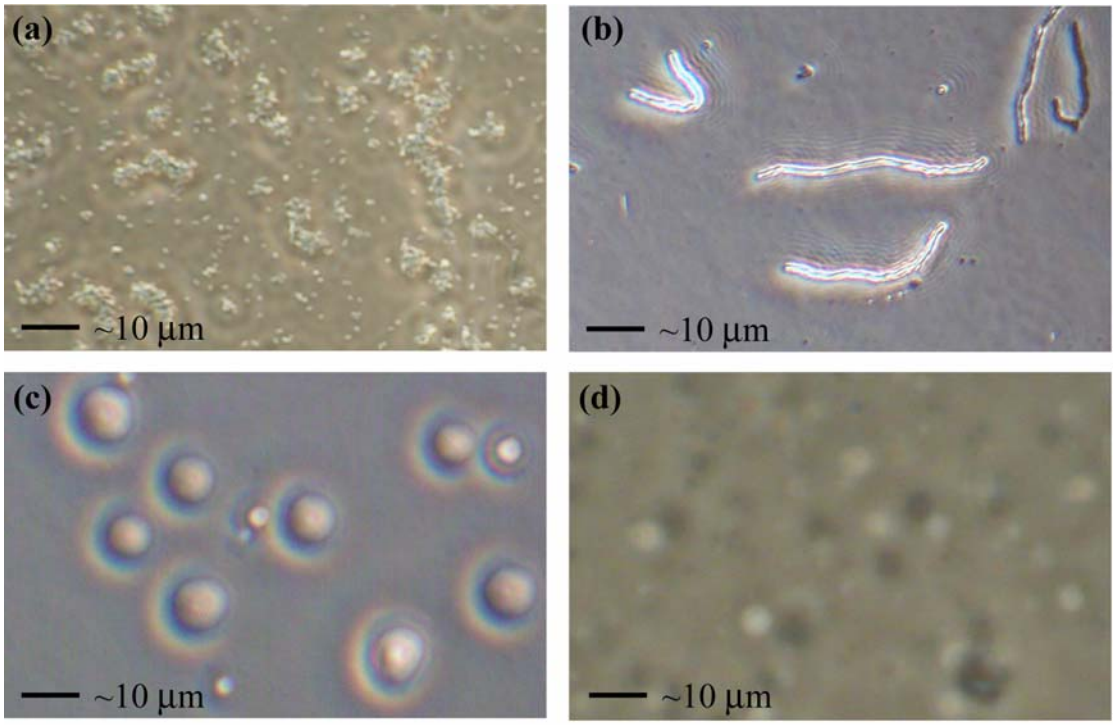

Figure 2.5. Generation of giant spheroplasts from *E. coli*. (A) *E. coli* culture, (B) "snakes" formed from cephalexin treatment, (C) healthy spheroplasts (D) unhealthy spheroplasts.

To generate spheroplasts, *E. coli* were cultured to an OD_{600} = 0.65 and then treated with cephalexin, an antibiotic that prevents septation but not the growth of the bacteria. The result is the formation of snake like strands of bacteria that are up to 100 µm in length (figure 2.5). Protein expression was induced in the snakes with the addition of isopropyl-β-D-thiogalactopyranoside (IPTG) and then the snakes were harvested and treated with lysozyme to digest the outer peptidoglycan layer of the snakes. Digestion with lysozyme forms the spheroplasts (Figure 2.5 (c)).

Spheroplast formation was highly inconsistent, such that less than 10% of the preparations yielded spheroplasts that were suitable for patch formation. More often than not, the preparations yielded collapsed spheroplasts or very weak spheroplasts that could not withstand the pressure needed to form a proper gigaohm seal (figure 2.5(d)). Numerous

attempts to optimize the protocol were not successful and did not appear to increase the rate of success for spheroplasts formation. The parameters that were varied in the optimization were the cephalexin incubation time, IPTG induction time, lysozyme induction time, amount of lysozyme, and the sucrose composition of the sucrose in the filtering solution. The shaking speed during the formation of snakes was also varied.

We speculate that the triple null strain MscL/MscS/MscK used in these experiments results in compromised *E. coli* membranes making them less durable to the demands of the spheroplast preparation. Because of the difficulty encountered in the generation of the spheroplasts, the data set for the wildtype and Arg46Ala mutant MscS channels is not extensive.

2.3.2 Electrophysiological characterization of wildtype MscS

Initial efforts were aimed at characterizing wildtype MscS using patch electrophysiology. The MscS channel was overexpressed in *E. coli* and characterized by cell detached inside out patch clamp electrophysiology. Expression was carried out in the MJF465 strain which has the three mechanosensitive channels MscL, MscS, and MscK knocked out. This was to ensure that any mechanosensitive channel activity would be due to the expressed gene product of the transformed MscS plasmid. *E. coli* that had been transformed with the expression plasmid containing the gene encoding MscS were used to generate spheroplasts using established protocols with some modifications.

Spheroplasts expressing MscS were evaluated using cell detached inside out patch clamp electrophysiology under symmetric buffer conditions with a total salt concentration of 300 mM. Initially, patches were held at a constant membrane potential of 20 mV and

pressure was gradually applied using suction until channel activity was observed. It should be noted that the amount of suction, and therefore pressure, needed to elicit a response from the expressed wildtype MscS channel varied from patch to patch due to differences in patch formation and membrane integrity. Once the minimum amount of pressure needed to elicit a response was determined for a particular patch, the patch was subjected to a developed voltage protocol. A schematic of this protocol is shown in figure 2.6. The determined pressure minimum was applied and held constant for each voltage jump while the membrane potential was increased in intervals of 10 mV. The pressure and desired membrane potential were applied for a 10 s period followed by a 50 s "rest" interval followed by another application of pressure with the next increment of membrane potential.

The wildtype MscS channel produced a single channel conductance of 1.5 nS under the aforementioned patch clamp recording conditions. The wildtype MscS channel also

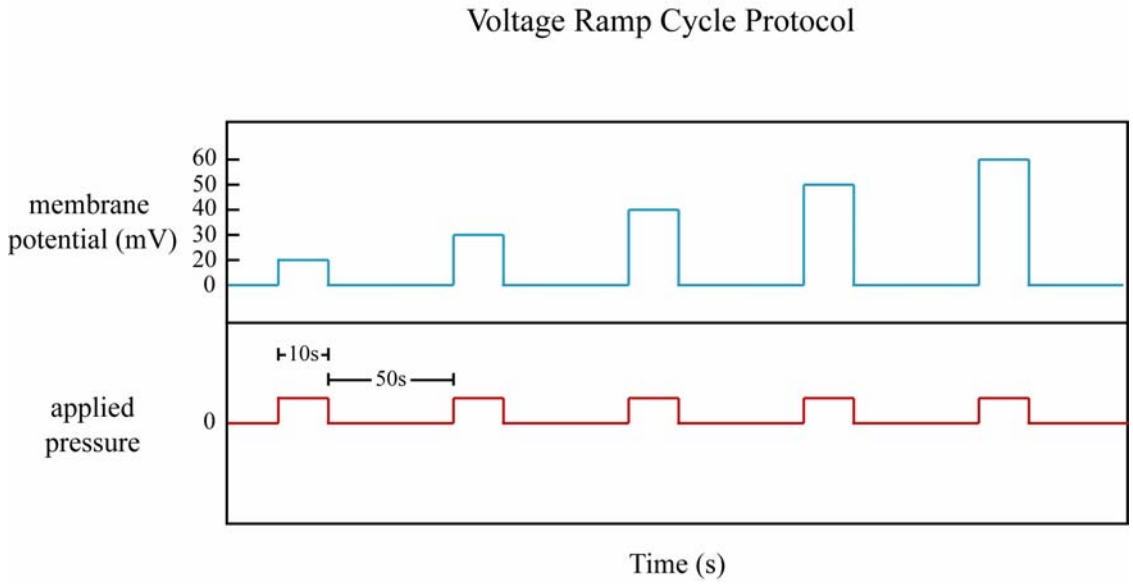

Figure 2.6. Schematic of voltage step protocol used for electrophysiological analysis of wildtype and mutant MscS.

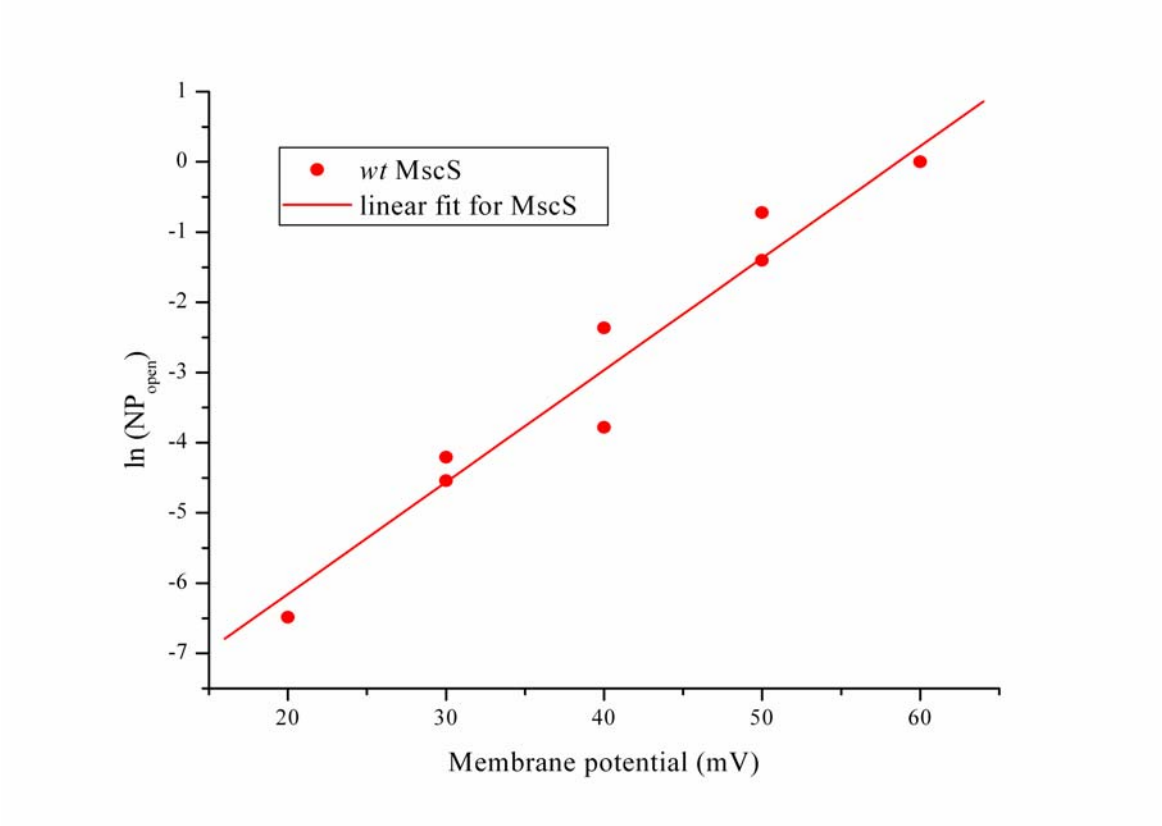

Figure 2.7. ln (NP_{open}) vs. membrane potential for *wildtype* MscS.

showed a strong dependence on voltage (figure 2.7) as observed by the open probability at various applied membrane potentials. At a constant applied pressure of 124 torr, the open probability, measured as $Np_{(open)}$, showed a linear log relationship with voltage (or applied membrane potential). Based on these initial measurements, an *e*-fold change in open probability occurs for every 6.44 mV change in voltage.

Interestingly, the activity of the wildtype MscS channels exhibited an unanticipated inactivation behavior. A successfully formed patch could only be evaluated with a single series of voltage steps before a significant loss of detected signal (figure 2.8). Application of multiple cycles of the voltage step protocol showed that the largest decrease in signal occurs after the first cycle and subsequent cycles show a much lower rate of signal decrease.

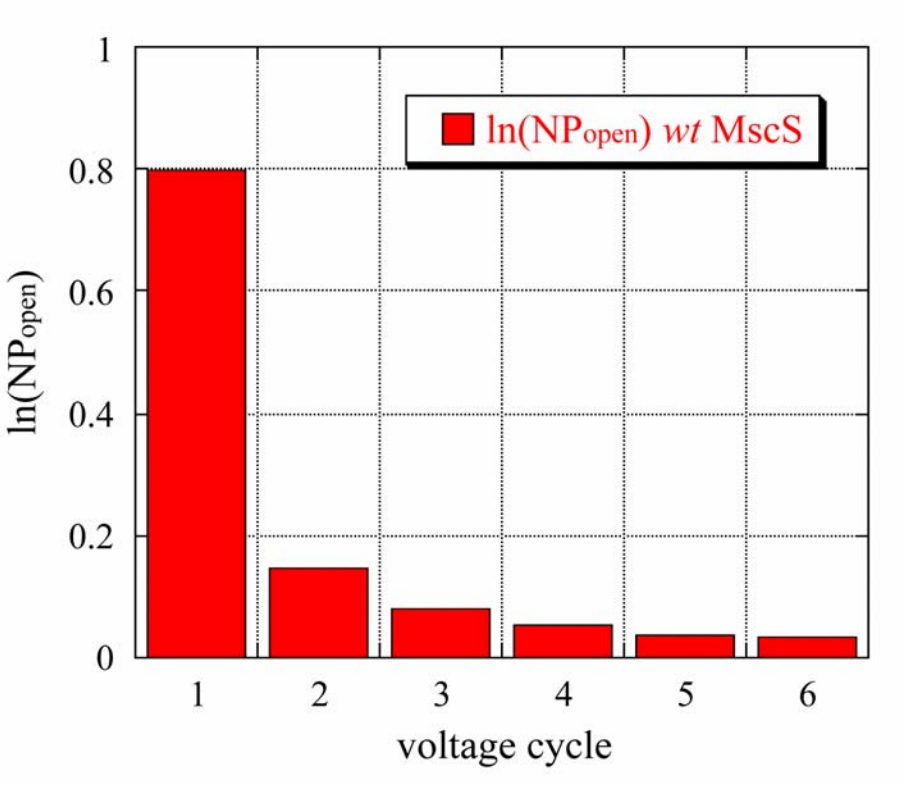

Figure 2.8. Wildtype MscS exhibits diminished activity after one cycle of the voltage step protocol.

2.3.3 Electrophysiological characterization of Arg46Ala mutant MscS

Arginine 46 in MscS was mutated to an alanine residue to determine the importance of arginine 46 in the voltage modulation of MscS. If arginine 46 is part of the voltage sensor of MscS, then neutralizing it should effectively remove or diminish the voltage sensitivity of the channel. Conventional site directed mutagenesis was used to generate the Arg46Ala mutant MscS which was then transformed into the MJF465 *E. coli* strain (Yan Poon, Rees Laboratory). Spheroplasts were generated using the transformed strain similar to the wildtype and subjected to electrophysiological analysis using patch clamp techniques. Successful patches containing the Arg46Ala mutant channels were subject to the same

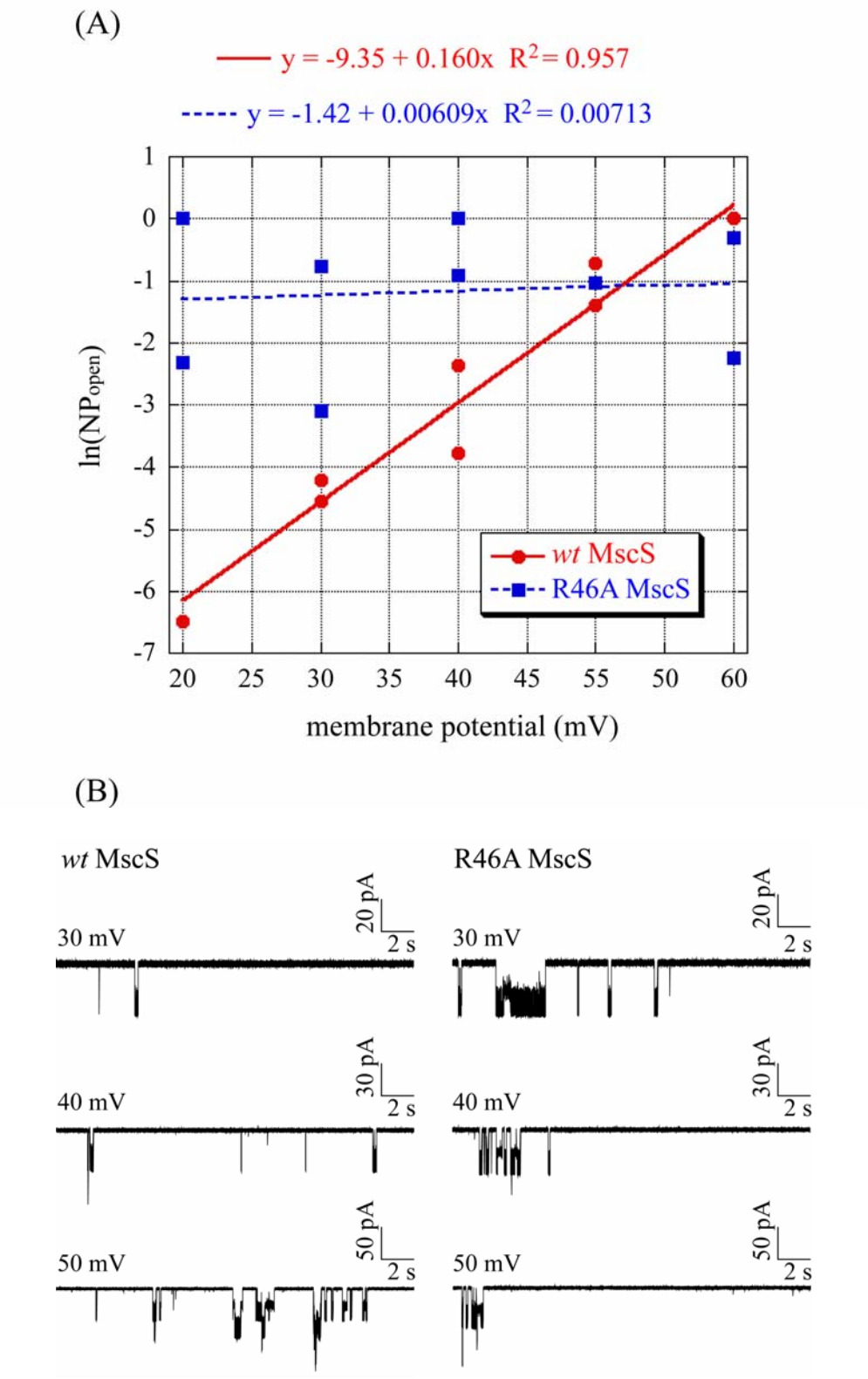

Figure 2.9. Comparison of $\ln(NP_{open})$ of wildtype MscS and Arg46Ala mutant MscS.

voltage protocol as the patches containing wildtype MscS channels, under the same bath conditions.

As seen in Figure 2.9, initial single channel recordings show no clear linear relationship between Np(open) and voltage for the Arg46Ala mutant MscS channel. The overall variation in Np(open) was significantly smaller than that of the wildtype. An attempted log fit of the data results in a very poor fit compared to that of the wildtype and the resulting slope is much less than for the wildtype. The mutant also differed from the wildtype MscS in several other interesting ways. The minimum pressure required to open the mutant channel at a membrane potential of +20 mV was 50% higher (186 torr) than that of the wildtype channel. Furthermore, the mutant channel did not exhibit the same drastic decrease in signal after the first series of voltage steps. A given successful patch containing Arg46Ala mutant MscS channels could be subjected to multiple cycles of the voltage step protocol without any significant decrease in channel signal (data not shown).

2.3.4. Characterization of Arg74Ala mutant MscS

Arginine 74 was mutated to an alanine residue and subjected the same analysis as the wildtype and Arg46Ala mutant MscS channels using patch clamp electrophysiology. Viable patches were formed from healthy spheroplasts, however all patches that were formed exhibited no channel activity. A substantial number of viable patches were tested, none of which exhibited channel activity. To ensure the channel was still properly expressed with the mutation at position 74, Western blot analysis of the membrane fraction was performed. As shown in Figure 2.10, both the Arg74Ala and Arg46Ala mutant MscS channels showed expression levels comparable to that of the wildtype.

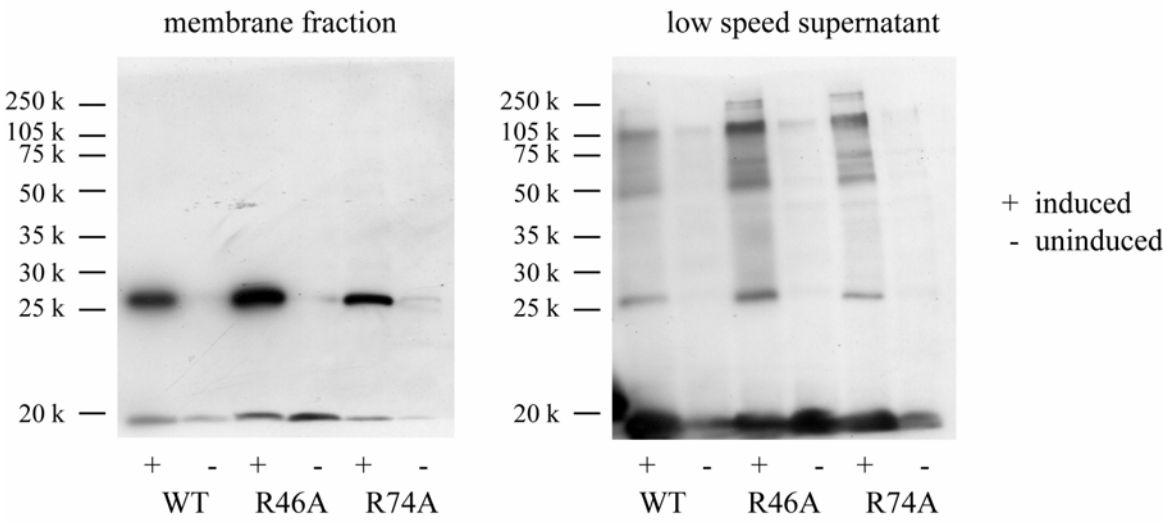

Figure 2.10. Western blot analysis of *wildtype* and mutant MscS expression levels from the membrane fraction (left) and the supernatant recovered after low speed centrifugation (right).

2.4 Discussion

Voltage-gated ion channels have been of great interest for biophysical studies since they were first detected by Hodgkin and Huxley. Decades of biophysical studies resulted in the proposed "helical screw" model for the mechanism of gating for voltage-gated ion channels. The controversial "paddle" model was proposed by MacKinnon *et al.* with the structure of K_vAP in 2003. This model differs considerably from the helical screw model and as such, intense interest continues to surround the field of voltage-gated ion channels. While MscS is not a typical voltage-gated ion channel, it shares some features that make it an attractive system to study that may lead to some insight into the mechanism of gating of voltage-gated ion channels. In particular, two arginine residues at position 46 and 74, located in TM1 and TM2 respectively, point out into the lipid membrane making them ideally placed to serve as voltage sensors during the gating process. Consequently the focus of the described work was aimed at elucidating the role of these arginines in the voltage-modulated

gating of MscS using single channel analysis with patch clamp electrophysiology in *E. coli* spheroplasts.

Our preliminary data indicated a strong voltage dependence for the wildtype MscS channel as compared to the R46A mutant MscS channel, which showed no apparent dependence on voltage. These results suggested that Arg46 plays a critical role in the voltage sensitivity of MscS since neutralization of this residue, by mutation to an alanine, removed or significantly reduced the voltage sensitivity. Additionally, computational work done by Spronk *et al.*, suggests that Arg46 and Arg74 are important for channel function.[106] Furthermore, this mutant channel also required a 50% higher minimum applied pressure to achieve comparable open probabilities to the wildtype. We also observed an inactivation behavior for the wildtype which was not seen with the R46A mutant channel. Based on these preliminary data, the wildtype channel indicated an *e*-fold change in Np(open) for every 6.44 mV change of transmembrane potential. Earlier work by Martinac *et al.*, suggested an *e*-fold change for every 15 mV change. The Arg74Ala mutant MscS channel exhibited no apparent channel activity despite healthy spheroplast and viable patch formation. Western blot analysis suggested the lack of channel activity was not due to lack of expression of the mutant channel.

These studies were greatly hampered by the inconsistent yield for the spheroplasts preparation. Less than 10% of the preparations yielded healthy spheroplasts that could form viable patches for electrophysiological analysis. Furthermore, the unanticipated inactivation behavior observed for the wildtype MscS channel also established another obstacle in obtaining a more extensive data set. It should also be noted that similar work performed by

Dr. Daniel A. Clayton yielded varying results in which the Arg46Ala mutant exhibited no apparent voltage dependence.

2.5 Conclusions

The research discussed herein was aimed at elucidating the role of two arginine residues in the TM1 and TM2 of MscS, a mechanosensitive ion channel that is also voltage-modulated. The MscS crystal structure reveals that these two arginines are appropriately positioned, pointing into the membrane, such that they could act as voltage sensors during gating. We generated two MscS mutants, Arg46Ala and Arg74Ala, to evaluate the effects of "neutralizing" the charged side chain on the voltage sensing ability of the channel. Using cell detached inside out patch clamp electrophysiology in *E. coli* spheroplasts, we evaluated the mutant channels and compared them to the wildtype MscS. Our preliminary results indicated a potentially significant role for Arg46 in the voltage sensitivity of MscS.

2.6 Experimental methods and materials

2.6.1 General

Unless otherwise stated, all reagents were purchased from commercial sources and used as is. MJF465 cells were received as a generous gift from Ian Booth. Site directed mutagenesis was performed by Yan Poon (Rees Laboratory) to generate the MscS mutants.

2.6.2 Electroporation of MJF465 cells with pB10b vector containing MscS

1 μL of mini-prep DNA expression plasmid was mixed with a 40 μL aliquot of MJF465 cells (MscL/MscS/MscK null *E. coli* strain). The MJF465 cells were thawed on ice

for 10 min prior to use. The cells and DNA mixture were mixed by gentle pipetting and then loaded into a 0.1 cm electroporation cuvette. The cuvettes were stored at –20 °C until needed. The cell and DNA mixture was then electroporated at 1800 V. A time constant in the range of 4.2 to 5.0 typically yielded efficiently transformed colonies. The cells were "rescued" with the addition of 0.5 mL of SOC media that had been warmed to 37 °C. The cells were mixed by gentle pipeting followed by transfer to a falcon culture tube. The culture was then incubated at 37 °C with shaking (300 rpm) for 15 to 20 min. The rescued culture was then plated on to LB-agar supplemented with ampicillin. 50 mL to 100 mL of culture was used per plate. Plates were incubated upside down at 37 °C for 10 h or until distinct colonies were observed. Colonies were then picked when needed to inoculate cultures.

2.6.3 Spheroplasts Preparation

A single colony or a perma-culture of a desired transformed *E. coli* strain was used to inoculate a 2 mL LB culture supplemented with ampicillin (0.1 μg/mL) (LB amp (+)) which was incubated at 37 °C with shaking at 300 rpm overnight (10 to 14 h) to produce a saturated culture. An aliquot (100 μL) of the saturated culture was removed and used to inoculate a 25 mL LB amp (+) culture. The culture was incubated at 37 °C and 300 rpm until the OD_{600} = 0.65, as measured by UV-vis spectroscopy. Subsequently, 5 mL of the 25 mL culture was added to a 50 mL LB amp (+) culture. To this culture was added 5.4 mg of cephalexin which was then incubated at 37 °C with shaking at 300 rpm for 1.5 h. Protein expression was induced by the addition of 0.5 mL of 100 mM IPTG and incubation was continued at 37 °C, 300 rpm for 15 min. The resulting snakes were aliquoted in 1 mL portions in eppendorfs and then harvested by centrifugation at 1500 x g for 15 min. at 4 °C. The supernatant was

decanted and the cell pellets were kept on ice during all subsequent steps unless otherwise noted. A 0.8 M sucrose solution (1 mL) was gently layered over each cell pellet without disturbing the pellet. The pellet was incubated on ice for 1 min. The sucrose solution was then gently removed and a fresh portion of 0.8 M sucrose (1 mL) was added. The pellet was gently resuspended by shaking. Vortexing was avoided. The resuspension was transferred to a glass test tube (10 x 75 mm). To each resuspension was added, in the following order with agitation: 1 M Tris-HCl, pH 7.8 (62.5 μL), 5 mg/mL lysozyme solution (60 μL) or lysonase (1 μL), 10 mg/mL DNAse (7.5 μL), and 0.5 M EDTA, pH 8.0 (18.75 μL). The reaction was incubated at room temperature with agitation (shake with hands) for 2-5 min. Reactions were monitored using light microscopy. Digestion reactions were terminated by the dropwise (with agitation) addition of 0.5 mL of "stop solution" (0.7 M sucrose, 20 mM $MgCl_2$, 10 mM Tris, pH 7.8). The terminated reaction was carefully layered on 10 mL of "filtering solution" (0.8 M sucrose, 10 mM $MgCl_2$, 10 mM Tris-HCl, pH 8.0) and subsequently centrifuged at 800 x g at 4 °C for 3 min. Each layer and partition was examined by microscropy to determine the presence of properly formed spheroplasts. The layers containing spheroplasts were harvested and aliquoted. Aliquots were promptly stored at -20 °C. When needed aliquots were thawed on ice.

During attempts to optimize this protocol the following parameters were varied: the cephalexin incubation time, IPTG induction time, lysozyme reaction time, lysonase amounts and reaction times, sucrose concentration in filtering solution, as well as the shaking speed during cephalexin incubation.

2.6.4 Electrophysiological characterization of MscS

The MscS channel was characterized by electrophysiology using the inside-out cell-detached patch clamp method. *E. coli* strain MJF465 ($MscL^-MscS^-MscK^-$) was used for all analysis. Spheroplasts expressing MscS were generated using an established protocol, and the channels were evaluated under symmetric buffer conditions (200 mM KCl, 90 mM $MgCl_2$, 100 mM $CaCl_2$, 15 mM HEPES, pH 7.5). Electrodes were pulled from borosilicate capillary tubes (World Precision Instruments, Sarasota, FL) using a micropipette puller (Model P-80/PC, Sutter Instruments, Novato CA). They were subsequently fire polished (MF-83, Narishige Scientific Instrument Lab, Tokyo, Japan) to give a pipette resistance of ~6 GΩ in recording solution. Negative pressure was applied through a syringe and measured by a calibrated pressure transducer (Omega Engineering, Stamford, CT). Currents were acquired with an AxoPatch 1-D amplifier (Axon Instruments) at a sampling rate of 25 kHz, filtered at 5 kHz and analyzed using pCLAMP9.0 software (Axon Instruments). All measurements were acquired from at least two spheroplasts preparations.

2.6.5 Membrane fraction isolation

An *E. coli* colony of the desired transformed strain was used to inoculate a 2 mL LB culture supplemented with ampicillin (0.1 μg/mL**)** (LB-amp +). The 2 mL culture was incubated overnight at 37 °C with shaking at (300 rpm) for 12 to 14 h to produce a saturated culture. 200 mL of the saturated culture was used to inoculate 50 mL of LB-amp (+) culture which was then incubated at 37 °C with shaking (300 rpm) until the OD_{600} = 0.6 to 0.8. Cephalexin (5.4 mg) was added to the culture which was then incubated for 1.5 hours to generate "snakes." Subsequently, 500 μL of 100 mM IPTG was added to induce protein

expression. Induction was allowed to proceed for 2 h at 37 °C with shaking (300 rpm). The resulting "snakes" were harvested by centrifugation, in pre-weighed centrifugation vessels, at 2000 x g for 10 min at 4 °C. The supernatant was decanted and the weight of the cell pellet was determined. Lysis buffer (5 mM EDTA, 50 mM Tris pH 7.5, 200 mM NaCl) was then added at the ratio of 200 mL of lysis buffer for every 25 g of cell pellet. Prior to resuspension and lysis, protease inhibitors (10 μg/mL), DNAse (1 mM), and lysozyme were added (5 μg/mL). $MgCl_2$ was added to a final concentration of 2 mM (add 2 μL of 1M $MgCl_2$ per 1 mL lysis buffer). The mixture was then sonicated to resuspend and the cell pellet. A probe sonicator with a microtip was used and sonication was performed on ice for a total of 15 s in 1 s sonication intervals with 10 s rest intervals to prevent overheating of the samples. The cell lysate was then centrifuged at 11,000 x g for 20 min at 4 °C. The low-speed supernatant was removed and saved and the pellet was resuspended in a volume of buffer equivalent to the volume of low-speed supernatant recovered (i.e., if there was 3 mL of supernatant, pellet was resuspended in 3 mL of buffer). This was done to normalize the volumes to allow for a direct comparison of Western blot analysis. A small portion (10 μL) of the low speed supernatant was reserved for Western blot analysis and then the remaining low speed supernatant was centrifuged at 150,000 x g for 1 hr. at 4 ºC to pellet the membranes. The high-speed supernatant was removed and saved and the resulting pellet was resuspended using normalizing volumes as before. The low-speed supernatant, high-speed supernatant, and pellet fraction were then subject to resolution by SDS-PAGE followed by Western blot analysis.

2.7 *References*

1. Tavernarakis, N.; Driscoll, M., Molecular modeling of mechanotransduction in the nematode Caenorhabditis elegans. *Annu Rev Physiol* **1997,** 59, 659-89.
2. Nakamura, F.; Strittmatter, S. M., P2Y1 purinergic receptors in sensory neurons: contribution to touch-induced impulse generation. *Proc Natl Acad Sci U S A* **1996,** 93, (19), 10465-70.
3. Burnstock, G.; Wood, J. N., Purinergic receptors: their role in nociception and primary afferent neurotransmission. *Curr Opin Neurobiol* **1996,** 6, (4), 526-32.
4. Burnstock, G., Release of vasoactive substances from endothelial cells by shear stress and purinergic mechanosensory transduction. *J Anat* **1999,** 194 (Pt 3), 335-42.
5. Howard, J.; Roberts, W. M.; Hudspeth, A. J., Mechanoelectrical transduction by hair cells. *Annu Rev Biophys Biophys Chem* **1988,** 17, 99-124.
6. Hackney, C. M.; Furness, D. N.; Benos, D. J.; Woodley, J. F.; Barratt, J., Putative immunolocalization of the mechanoelectrical transduction channels in mammalian cochlear hair cells. *Proc Biol Sci* **1992,** 248, (1323), 215-21.
7. Hackney, C. M.; Furness, D. N., Mechanotransduction in vertebrate hair cells: structure and function of the stereociliary bundle. *Am J Physiol* **1995,** 268, (1 Pt 1), C1-13.
8. Duncan, R. L.; Turner, C. H., Mechanotransduction and the functional response of bone to mechanical strain. *Calcif Tissue Int* **1995,** 57, (5), 344-58.
9. Wang, Y.; Roman, R.; Lidofsky, S. D.; Fitz, J. G., Autocrine signaling through ATP release represents a novel mechanism for cell volume regulation. *Proc Natl Acad Sci U S A* **1996,** 93, (21), 12020-5.
10. Okada, Y., Volume expansion-sensing outward-rectifier Cl- channel: fresh start to the molecular identity and volume sensor. *Am J Physiol* **1997,** 273, (3 Pt 1), C755-89.
11. Nilius, B.; Eggermont, J.; Voets, T.; Buyse, G.; Manolopoulos, V.; Droogmans, G., Properties of volume-regulated anion channels in mammalian cells. *Prog Biophys Mol Biol* **1997,** 68, (1), 69-119.
12. Gustin, M. C.; Zhou, X. L.; Martinac, B.; Kung, C., A mechanosensitive ion channel in the yeast plasma membrane. *Science* **1988,** 242, (4879), 762-5.
13. Franco, A., Jr.; Lansman, J. B., Calcium entry through stretch-inactivated ion channels in mdx myotubes. *Nature* **1990,** 344, (6267), 670-3.
14. Driscoll, M.; Chalfie, M., The mec-4 gene is a member of a family of Caenorhabditis elegans genes that can mutate to induce neuronal degeneration. *Nature* **1991,** 349, (6310), 588-93.
15. Hansen, D. E.; Craig, C. S.; Hondeghem, L. M., Stretch-induced arrhythmias in the isolated canine ventricle. Evidence for the importance of mechanoelectrical feedback. *Circulation* **1990,** 81, (3), 1094-105.
16. Franz, M. R.; Cima, R.; Wang, D.; Profitt, D.; Kurz, R., Electrophysiological effects of myocardial stretch and mechanical determinants of stretch-activated arrhythmias. *Circulation* **1992,** 86, (3), 968-78.
17. Dean, J. W.; Lab, M. J., Arrhythmia in heart failure: role of mechanically induced changes in electrophysiology. *Lancet* **1989,** 1, (8650), 1309-12.
18. Kohler, R.; Distler, A.; Hoyer, J., Increased mechanosensitive currents in aortic endothelial cells from genetically hypertensive rats. *J Hypertens* **1999,** 17, (3), 365-71.

19. Dimmeler, S.; Hermann, C.; Zeiher, A. M., Apoptosis of endothelial cells. Contribution to the pathophysiology of atherosclerosis? *Eur Cytokine Netw* **1998,** 9, (4), 697-8.
20. Mitchell, C. H.; Carre, D. A.; McGlinn, A. M.; Stone, R. A.; Civan, M. M., A release mechanism for stored ATP in ocular ciliary epithelial cells. *Proc Natl Acad Sci U S A* **1998,** 95, (12), 7174-8.
21. Morris, C. E., Mechanosensitive ion channels. *J Membr Biol* **1990,** 113, (2), 93-107.
22. Sukharev, S. I.; Blount, P.; Martinac, B.; Kung, C., Mechanosensitive channels of Escherichia coli: the MscL gene, protein, and activities. *Annu Rev Physiol* **1997,** 59, 633-57.
23. Martinac, B., Mechanosensitive channels in prokaryotes. *Cell Physiol Biochem* **2001,** 11, (2), 61-76.
24. Casado, M.; Ascher, P., Opposite modulation of NMDA receptors by lysophospholipids and arachidonic acid: common features with mechanosensitivity. *J Physiol* **1998,** 513 (Pt 2), 317-30.
25. Paoletti, P.; Ascher, P., Mechanosensitivity of NMDA receptors in cultured mouse central neurons. *Neuron* **1994,** 13, (3), 645-55.
26. Lehtonen, J. Y.; Kinnunen, P. K., Phospholipase A2 as a mechanosensor. *Biophys J* **1995,** 68, (5), 1888-94.
27. Matsumoto, H.; Baron, C. B.; Coburn, R. F., Smooth muscle stretch-activated phospholipase C activity. *Am J Physiol* **1995,** 268, (2 Pt 1), C458-65.
28. Chen, B. M.; Grinnell, A. D., Kinetics, Ca2+ dependence, and biophysical properties of integrin-mediated mechanical modulation of transmitter release from frog motor nerve terminals. *J Neurosci* **1997,** 17, (3), 904-16.
29. Gillespie, P. G.; Walker, R. G., Molecular basis of mechanosensory transduction. *Nature* **2001,** 413, (6852), 194-202.
30. Hamill, O. P.; Martinac, B., Molecular basis of mechanotransduction in living cells. *Physiol Rev* **2001,** 81, (2), 685-740.
31. Society of General Physiologists. Symposium (50th : 1996 Woods Hole Mass.); Froehner, S. C.; Bennett, V., *Cytoskeletal regulation of membrane function : Society of General Physiologists 50th annual symposium, Marine Biological Laboratory, Woods Hole, Massachusetts, 5-7 September 1996*. Rockefeller University Press: New York, 1997; p vii, 280 p.
32. Pivetti, C. D.; Yen, M. R.; Miller, S.; Busch, W.; Tseng, Y. H.; Booth, I. R.; Saier, M. H., Jr., Two families of mechanosensitive channel proteins. *Microbiol Mol Biol Rev* **2003,** 67, (1), 66-85, table of contents.
33. Clapham, D. E.; Runnels, L. W.; Strubing, C., The TRP ion channel family. *Nat Rev Neurosci* **2001,** 2, (6), 387-96.
34. Maingret, F.; Fosset, M.; Lesage, F.; Lazdunski, M.; Honore, E., TRAAK is a mammalian neuronal mechano-gated K+ channel. *J Biol Chem* **1999,** 274, (3), 1381-7.
35. Maingret, F.; Patel, A. J.; Lesage, F.; Lazdunski, M.; Honore, E., Mechano- or acid stimulation, two interactive modes of activation of the TREK-1 potassium channel. *J Biol Chem* **1999,** 274, (38), 26691-6.
36. Welsh, M. J.; Price, M. P.; Xie, J., Biochemical basis of touch perception: mechanosensory function of degenerin/epithelial Na+ channels. *J Biol Chem* **2002,** 277, (4), 2369-72.

37. Tavernarakis, N.; Driscoll, M., Mechanotransduction in Caenorhabditis elegans: the role of DEG/ENaC ion channels. *Cell Biochem Biophys* **2001,** 35, (1), 1-18.
38. Martinac, B.; Buechner, M.; Delcour, A. H.; Adler, J.; Kung, C., Pressure-sensitive ion channel in Escherichia coli. *Proc Natl Acad Sci U S A* **1987,** 84, (8), 2297-301.
39. Szabo, I.; Petronilli, V.; Zoratti, M., A patch-clamp investigation of the Streptococcus faecalis cell membrane. *J Membr Biol* **1993,** 131, (3), 203-18.
40. Zoratti, M.; Petronilli, V.; Szabo, I., Stretch-activated composite ion channels in Bacillus subtilis. *Biochem Biophys Res Commun* **1990,** 168, (2), 443-50.
41. Delcour, A. H.; Martinac, B.; Adler, J.; Kung, C., Voltage-sensitive ion channel of Escherichia coli. *J Membr Biol* **1989,** 112, (3), 267-75.
42. Le Dain, A. C.; Saint, N.; Kloda, A.; Ghazi, A.; Martinac, B., Mechanosensitive ion channels of the archaeon Haloferax volcanii. *J Biol Chem* **1998,** 273, (20), 12116-9.
43. Berrier, C.; Coulombe, A.; Houssin, C.; Ghazi, A., A patch-clamp study of ion channels of inner and outer membranes and of contact zones of E. coli, fused into giant liposomes. Pressure-activated channels are localized in the inner membrane. *FEBS Lett* **1989,** 259, (1), 27-32.
44. Sukharev, S. I.; Blount, P.; Martinac, B.; Blattner, F. R.; Kung, C., A large-conductance mechanosensitive channel in E. coli encoded by mscL alone. *Nature* **1994,** 368, (6468), 265-8.
45. Blount, P.; Sukharev, S. I.; Moe, P. C.; Martinac, B.; Kung, C., Mechanosensitive channels of bacteria. *Methods Enzymol* **1999,** 294, 458-82.
46. Sukharev, S., Mechanosensitive channels in bacteria as membrane tension reporters. *Faseb J* **1999,** 13 Suppl, S55-61.
47. Okada, K.; Moe, P. C.; Blount, P., Functional design of bacterial mechanosensitive channels. Comparisons and contrasts illuminated by random mutagenesis. *J Biol Chem* **2002,** 277, (31), 27682-8.
48. Sukharev, S., Purification of the small mechanosensitive channel of Escherichia coli (MscS): the subunit structure, conduction, and gating characteristics in liposomes. *Biophys J* **2002,** 83, (1), 290-8.
49. Li, Y.; Moe, P. C.; Chandrasekaran, S.; Booth, I. R.; Blount, P., Ionic regulation of MscK, a mechanosensitive channel from Escherichia coli. *Embo J* **2002,** 21, (20), 5323-30.
50. Kloda, A.; Martinac, B., Mechanosensitive channels of bacteria and archaea share a common ancestral origin. *Eur Biophys J* **2002,** 31, (1), 14-25.
51. Blount, P.; Moe, P. C., Bacterial mechanosensitive channels: integrating physiology, structure and function. *Trends Microbiol* **1999,** 7, (10), 420-4.
52. Levina, N.; Totemeyer, S.; Stokes, N. R.; Louis, P.; Jones, M. A.; Booth, I. R., Protection of Escherichia coli cells against extreme turgor by activation of MscS and MscL mechanosensitive channels: identification of genes required for MscS activity. *Embo J* **1999,** 18, (7), 1730-7.
53. Kloda, A.; Martinac, B., Common evolutionary origins of mechanosensitive ion channels in Archaea, Bacteria and cell-walled Eukarya. *Archaea* **2002,** 1, (1), 35-44.
54. Miller, S.; Bartlett, W.; Chandrasekaran, S.; Simpson, S.; Edwards, M.; Booth, I. R., Domain organization of the MscS mechanosensitive channel of Escherichia coli. *Embo J* **2003,** 22, (1), 36-46.

55. Bass, R. B.; Strop, P.; Barclay, M.; Rees, D. C., Crystal structure of Escherichia coli MscS, a voltage-modulated and mechanosensitive channel. *Science* **2002,** 298, (5598), 1582-7.
56. Hodgkin, A. L.; Huxley, A. F., Propagation of electrical signals along giant nerve fibers. *Proc R Soc Lond B Biol Sci* **1952,** 140, (899), 177-83.
57. Hodgkin, A. L.; Huxley, A. F., A quantitative description of membrane current and its application to conduction and excitation in nerve. *J Physiol* **1952,** 117, (4), 500-44.
58. Hodgkin, A. L.; Huxley, A. F., The dual effect of membrane potential on sodium conductance in the giant axon of Loligo. *J Physiol* **1952,** 116, (4), 497-506.
59. Hodgkin, A. L.; Huxley, A. F., The components of membrane conductance in the giant axon of Loligo. *J Physiol* **1952,** 116, (4), 473-96.
60. Hodgkin, A. L.; Huxley, A. F., Currents carried by sodium and potassium ions through the membrane of the giant axon of Loligo. *J Physiol* **1952,** 116, (4), 449-72.
61. Hodgkin, A. L.; Huxley, A. F., Movement of sodium and potassium ions during nervous activity. *Cold Spring Harb Symp Quant Biol* **1952,** 17, 43-52.
62. Hodgkin, A. L.; Huxley, A. F.; Katz, B., Measurement of current-voltage relations in the membrane of the giant axon of Loligo. *J Physiol* **1952,** 116, (4), 424-48.
63. Agnew, W. S.; Levinson, S. R.; Brabson, J. S.; Raftery, M. A., Purification of the tetrodotoxin-binding component associated with the voltage-sensitive sodium channel from Electrophorus electricus electroplax membranes. *Proc Natl Acad Sci U S A* **1978,** 75, (6), 2606-10.
64. Noda, M.; Shimizu, S.; Tanabe, T.; Takai, T.; Kayano, T.; Ikeda, T.; Takahashi, H.; Nakayama, H.; Kanaoka, Y.; Minamino, N.; et al., Primary structure of Electrophorus electricus sodium channel deduced from cDNA sequence. *Nature* **1984,** 312, (5990), 121-7.
65. Tempel, B. L.; Papazian, D. M.; Schwarz, T. L.; Jan, Y. N.; Jan, L. Y., Sequence of a probable potassium channel component encoded at Shaker locus of Drosophila. *Science* **1987,** 237, (4816), 770-5.
66. Doyle, D. A.; Morais Cabral, J.; Pfuetzner, R. A.; Kuo, A.; Gulbis, J. M.; Cohen, S. L.; Chait, B. T.; MacKinnon, R., The structure of the potassium channel: molecular basis of K+ conduction and selectivity. *Science* **1998,** 280, (5360), 69-77.
67. Zhou, Y.; Morais-Cabral, J. H.; Kaufman, A.; MacKinnon, R., Chemistry of ion coordination and hydration revealed by a K+ channel-Fab complex at 2.0 A resolution. *Nature* **2001,** 414, (6859), 43-8.
68. Morais-Cabral, J. H.; Zhou, Y.; MacKinnon, R., Energetic optimization of ion conduction rate by the K+ selectivity filter. *Nature* **2001,** 414, (6859), 37-42.
69. Berneche, S.; Roux, B., Energetics of ion conduction through the K+ channel. *Nature* **2001,** 414, (6859), 73-7.
70. Choe, S., Potassium channel structures. *Nat Rev Neurosci* **2002,** 3, (2), 115-21.
71. Sansom, M. S.; Shrivastava, I. H.; Bright, J. N.; Tate, J.; Capener, C. E.; Biggin, P. C., Potassium channels: structures, models, simulations. *Biochim Biophys Acta* **2002,** 1565, (2), 294-307.
72. Yellen, G., Permeation in potassium channels: implications for channel structure. *Annu Rev Biophys Biophys Chem* **1987,** 16, 227-46.
73. Corry, B.; Chung, S. H., Mechanisms of valence selectivity in biological ion channels. *Cell Mol Life Sci* **2006,** 63, (3), 301-15.

74. Kurata, H. T.; Fedida, D., A structural interpretation of voltage-gated potassium channel inactivation. *Prog Biophys Mol Biol* **2006,** 92, (2), 185-208.
75. Armstrong, C. M., Interaction of tetraethylammonium ion derivatives with the potassium channels of giant axons. *J Gen Physiol* **1971,** 58, (4), 413-37.
76. Holmgren, M.; Smith, P. L.; Yellen, G., Trapping of organic blockers by closing of voltage-dependent K+ channels: evidence for a trap door mechanism of activation gating. *J Gen Physiol* **1997,** 109, (5), 527-35.
77. Holmgren, M.; Shin, K. S.; Yellen, G., The activation gate of a voltage-gated K+ channel can be trapped in the open state by an intersubunit metal bridge. *Neuron* **1998,** 21, (3), 617-21.
78. del Camino, D.; Holmgren, M.; Liu, Y.; Yellen, G., Blocker protection in the pore of a voltage-gated K+ channel and its structural implications. *Nature* **2000,** 403, (6767), 321-5.
79. del Camino, D.; Yellen, G., Tight steric closure at the intracellular activation gate of a voltage-gated K(+) channel. *Neuron* **2001,** 32, (4), 649-56.
80. Antz, C.; Bauer, T.; Kalbacher, H.; Frank, R.; Covarrubias, M.; Kalbitzer, H. R.; Ruppersberg, J. P.; Baukrowitz, T.; Fakler, B., Control of K+ channel gating by protein phosphorylation: structural switches of the inactivation gate. *Nat Struct Biol* **1999,** 6, (2), 146-50.
81. Murrell-Lagnado, R. D.; Aldrich, R. W., Energetics of Shaker K channels block by inactivation peptides. *J Gen Physiol* **1993,** 102, (6), 977-1003.
82. Murrell-Lagnado, R. D.; Aldrich, R. W., Interactions of amino terminal domains of Shaker K channels with a pore blocking site studied with synthetic peptides. *J Gen Physiol* **1993,** 102, (6), 949-75.
83. Zagotta, W. N.; Hoshi, T.; Aldrich, R. W., Restoration of inactivation in mutants of Shaker potassium channels by a peptide derived from ShB. *Science* **1990,** 250, (4980), 568-71.
84. Aldrich, R. W., Fifty years of inactivation. *Nature* **2001,** 411, (6838), 643-4.
85. Hoshi, T.; Zagotta, W. N.; Aldrich, R. W., Two types of inactivation in Shaker K+ channels: effects of alterations in the carboxy-terminal region. *Neuron* **1991,** 7, (4), 547-56.
86. Liu, Y.; Jurman, M. E.; Yellen, G., Dynamic rearrangement of the outer mouth of a K+ channel during gating. *Neuron* **1996,** 16, (4), 859-67.
87. Ruppersberg, J. P.; Stocker, M.; Pongs, O.; Heinemann, S. H.; Frank, R.; Koenen, M., Regulation of fast inactivation of cloned mammalian IK(A) channels by cysteine oxidation. *Nature* **1991,** 352, (6337), 711-4.
88. Yellen, G.; Sodickson, D.; Chen, T. Y.; Jurman, M. E., An engineered cysteine in the external mouth of a K+ channel allows inactivation to be modulated by metal binding. *Biophys J* **1994,** 66, (4), 1068-75.
89. Hoshi, T.; Zagotta, W. N.; Aldrich, R. W., Biophysical and molecular mechanisms of Shaker potassium channel inactivation. *Science* **1990,** 250, (4980), 533-8.
90. Choi, K. L.; Aldrich, R. W.; Yellen, G., Tetraethylammonium blockade distinguishes two inactivation mechanisms in voltage-activated K+ channels. *Proc Natl Acad Sci U S A* **1991,** 88, (12), 5092-5.
91. Tombola, F.; Pathak, M. M.; Isacoff, E. Y., How Does Voltage Open an Ion Channel? *Annu Rev Cell Dev Biol* **2006,** 22, 23-52.
92. Bezanilla, F., Voltage sensor movements. *J Gen Physiol* **2002,** 120, (4), 465-73.

93. Bezanilla, F., Voltage-gated ion channels. *IEEE Trans Nanobioscience* **2005,** 4, (1), 34-48.
94. Bezanilla, F.; Perozo, E., Structural biology. Force and voltage sensors in one structure. *Science* **2002,** 298, (5598), 1562-3.
95. Durell, S. R.; Guy, H. R., Atomic scale structure and functional models of voltage-gated potassium channels. *Biophys J* **1992,** 62, (1), 238-47; discussion 247-50.
96. Gandhi, C. S.; Isacoff, E. Y., Molecular models of voltage sensing. *J Gen Physiol* **2002,** 120, (4), 455-63.
97. Durell, S. R.; Shrivastava, I. H.; Guy, H. R., Models of the structure and voltage-gating mechanism of the shaker K+ channel. *Biophys J* **2004,** 87, (4), 2116-30.
98. Catterall, W. A., Molecular properties of voltage-sensitive sodium channels. *Annu Rev Biochem* **1986,** 55, 953-85.
99. Ahern, C. A.; Horn, R., Specificity of charge-carrying residues in the voltage sensor of potassium channels. *J Gen Physiol* **2004,** 123, (3), 205-16.
100. Starace, D. M.; Bezanilla, F., A proton pore in a potassium channel voltage sensor reveals a focused electric field. *Nature* **2004,** 427, (6974), 548-53.
101. Jiang, Y.; Lee, A.; Chen, J.; Ruta, V.; Cadene, M.; Chait, B. T.; MacKinnon, R., X-ray structure of a voltage-dependent K+ channel. *Nature* **2003,** 423, (6935), 33-41.
102. Jiang, Y.; Ruta, V.; Chen, J.; Lee, A.; MacKinnon, R., The principle of gating charge movement in a voltage-dependent K+ channel. *Nature* **2003,** 423, (6935), 42-8.
103. Cohen, B. E.; Grabe, M.; Jan, L. Y., Answers and questions from the KvAP structures. *Neuron* **2003,** 39, (3), 395-400.
104. Miller, C., A charged view of voltage-gated ion channels. *Nat Struct Biol* **2003,** 10, (6), 422-4.
105. Ruthe, H. J.; Adler, J., Fusion of bacterial spheroplasts by electric fields. *Biochim Biophys Acta* **1985,** 819, (1), 105-13.
106. Spronk, S. A.; Elmore, D. E.; Dougherty, D. A., Voltage-dependent hydration and conduction properties of the hydrophobic pore of the mechanosensitive channel of small conductance. *Biophys J* **2006,** 90, (10), 3555-69.